Slow light engineering in periodic-stub-assisted plasmonic waveguide

Guoxi Wang

State Key Laboratory of Transient Optics and Photonics, Xi'an Institute of Optics and Precision Mechanics, Chinese Academy of Sciences, Xi'an 710119, China (wangguoxi@opt.cn)

Received 28 November 2012; revised 31 January 2013; accepted 13 February 2013; posted 14 February 2013 (Doc. ID 180813); published 12 March 2013

We investigate the slow light engineering in periodic-stub-assisted plasmonic waveguide based on transmission line theory. It is found that the dispersion relationship of the proposed waveguide can be easily modified by tuning the stub depth and the period. The theoretical results show that a large normalized delay bandwidth product of 0.65 can be achieved at 1550 nm, meanwhile maintaining the group index of 35. In addition, the proposed waveguide shows "S-shaped" dispersion curve, which implies that the group velocity dispersion parameter at the inflection point equals zero and a dispersion-free slow light waveguide can be realized. Due to the excellent buffering capacity, the proposed compact configuration can find important applications on optical buffers in highly integrated optical circuits. © 2013 Optical Society of America

OCIS codes: 240.6680, 200.4490, 130.3120.

1. Introduction

Slowing down the propagation speed of light, and to coherently trap and store optical pulses, has drawn a lot of attention for its profound applications in optical communication and quantum information processing [1]. Several important approaches, including quantum interference effects or electromagnetically induced transparency (EIT) [2–4], photonic crystal waveguide [5,6], and stimulated Brillouin or Raman scattering [7], have been proposed to generate slow light. Recently, a lot of structures have been reported to realize slow light effect [8–15]. Among these structures, metal–insulator–metal (MIM) waveguides have attracted much attention for the better confinement of light with an acceptable propagation length for surface plasmon polaritons (SPPs) [16–20]. Some important nanoscale devices based on MIM waveguides have been recently reported, such as demultiplexers [16,17], reflectors [19], all-optical switches [21,22], and filters [23].

Though slow light effect can be realized in MIM waveguide [20], the normalized delay bandwidth product (NDBP) is very low. The NDBP is an important index that indicates the buffering capacity of the slow light devices [5]. The low NDBP means the poor buffering capacity of the proposed slow light waveguide. The low NDBP can be attributed to the low group index and the narrow bandwidth of the plasmonic slow light waveguide. However, it does not mean low NDBP is the feature of the plasmonic waveguide. In fact, by optimizing the geometrical parameters, the low NDBP can be improved significantly. In addition, the slow light in plasmonic waveguide is usually accompanied by the large group velocity dispersion (GVD) parameter. That is because slow light can usually be observed close to the photonic bandgap of the proposed slow light waveguide and the dispersion relationship around the slow light operating point shows a near parabolic characteristic. The large GVD parameter can result in the pulse distortion, which severely limits the applications of the plasmonic slow light waveguide. So it is highly important to investigate and improve the NDBP and reduce the GVD parameter of plasmonic slow light waveguide. As well known, the dispersion effect

1559-128X/13/091799-06$15.00/0

is one of the features of the periodic plasmonic waveguide and the dispersion of the plasmonic slow light waveguide can be attributed to two parts: the material dispersion and the grating-induced dispersion [24]. In MIM waveguide, the metal cladding is quite dispersive, so grating-induced dispersion should be carefully designed to compensate the metal-induced dispersion. Therefore, it is necessary to investigate the relationship between the structure-induced dispersion and the geometric parameters.

In this paper, we aim to solve two problems: one is to investigate the relationship between the dispersion and the geometric parameters of the proposed waveguide and the other is to improve the NDBP and reduce the GVD parameter of the plasmonic slow light waveguide. As we know, the NDBP is determined by the average group index and the bandwidth. So we studied the relationship between the dispersion and the geometric parameters of the proposed waveguide to get a flat dispersion curve and a large bandwidth. By optimizing the geometric parameters of the slow light waveguide, a large NDBP of 0.65 can be achieved. In addition, different from previous reports that usually generated slow light at the photonic bandgap edge, we propose a novel slow light waveguide based on a plasmonic analog of EIT. By using transmission line theory, we find that the proposed waveguide shows "S-shaped" dispersion curve, which indicates that at the inflection point of the dispersion curve, the GVD parameter equals zero. Our results provide important theoretical basis for the designs of the flat band plasmonic slow light devices.

2. Structure Model and Theory

Figure 1 shows the schematic diagram of the proposed plasmonic waveguide, which is composed of a MIM waveguide coupled with plasmonic grating. Each unit of the grating consists of two stubs with different depths. When a TM-polarized plane-wave is coupled into the waveguide, SPP wave can be excited at the metal–insulator interfaces and confined in the insulator layer. The metal in the proposed structure is selected as silver, whose frequency-dependent relative permittivity is characterized by the Drude model [25–27]:

$$\varepsilon_m(\omega) = \varepsilon_\infty - \frac{\omega_p^2}{\omega(\omega + i\gamma)}, \tag{1}$$

where ε_∞ is the dielectric constant at infinite angular frequency, ω_p is the bulk plasma frequency, and γ is the electron collision frequency. ω is the angular frequency of the incident wave in vacuum. The values of these parameters can be set as $\varepsilon_\infty = 3.7$, $\omega_p = 9.1$ eV, $\gamma = 0.018$ eV [28,29].

Here, we use an improved transmission model [30] and transmission line theory [31] to account for the transmission and dispersion properties of the plasmonic slow light waveguide. According to the transmission line theory, the plasmonic waveguide can be described by using the analog of a parallel connection of an infinite transmission line and serial finite microwave transmission line. With this analogy, each stub is equivalent to an open-circuited transmission line with effective impedance described by $Z_{\text{stub}} = Z_s(Z_L - iZ_s \tan(\beta_s h))/(Z_s - iZ_L \tan(\beta_s h))$, where $Z_s = \beta_s w/\omega\varepsilon_0\varepsilon_{\text{air}}$ and $Z_L = (\varepsilon_m/\varepsilon_{\text{air}})^{1/2} Z_s$. $\beta_0(\beta_s)$ is the propagation constant of the fundamental propagating TM mode in MIM waveguide (stub), h is the depth of the stub. With the above transmission line model, the transmission of each unit of the proposed structure is given by $T = T_{\text{MIM}} T_{\text{stub1}} T_{\text{stub2}} T_{\text{MIM}}$ with:

$$T_{\text{MIM}} = \begin{pmatrix} \exp(-i\beta_0 p) & 0 \\ 0 & \exp(i\beta_0 p) \end{pmatrix},$$
$$T_{\text{stub}} = \begin{pmatrix} 1 + \frac{Z_{\text{MIM}}}{2Z_{\text{stub}}} & \frac{Z_{\text{MIM}}}{2Z_{\text{stub}}} \\ -\frac{Z_{\text{MIM}}}{2Z_{\text{stub}}} & 1 - \frac{Z_{\text{MIM}}}{2Z_{\text{stub}}} \end{pmatrix}, \tag{2}$$

here, $Z_{\text{MIM}} = \beta_0 w/\omega\varepsilon_0\varepsilon_{\text{air}}$ is characteristic impedance of the MIM line, the transfer matrix T_{MIM} describes wave propagation between the stub and input/output facet of the waveguide, while the matrix T_{stub1} (T_{stub2}) represents coupling between the forward- and backward-propagating waves caused by

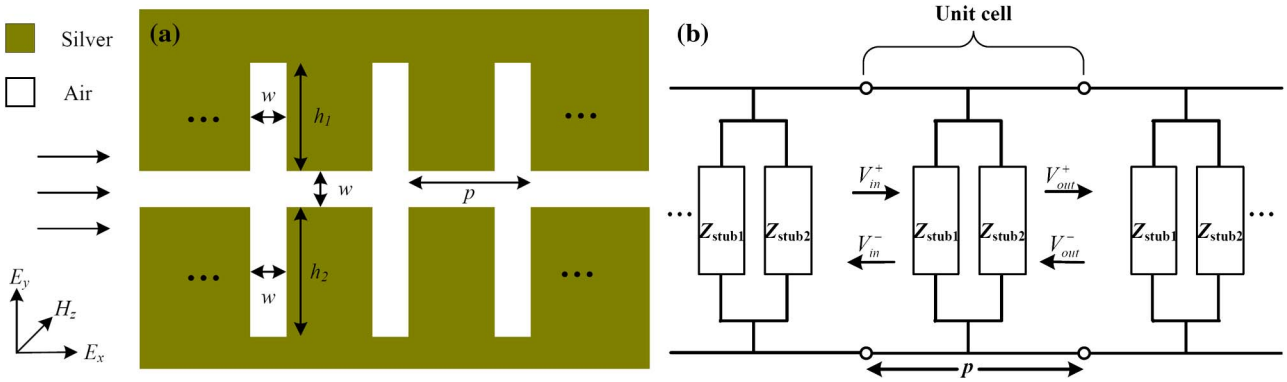

Fig. 1. (Color online) (a) Schematic of the MIM plasmonic waveguide: w, the width of the waveguide and stubs; p, the period of the grating; h_1 (h_2) the depth of the upper (lower) stubs. (b) Equivalent circuit of the proposed MIM waveguide system.

impedance $Z_{stub1}(Z_{stub2})$. When the MIM waveguide is coupled with N units, the transmission can be expressed as $T = (T_{MIM}T_{stub1}T_{stub2}T_{MIM})^N$. Then the Bloch wave dispersion relation for this periodic stub structure can be written as:

$$\cosh(Kp) = \frac{1}{2}(T_{11} + T_{22}), \tag{3}$$

where $K = \alpha + i\beta$ is the Bloch wave number of the entire system and T_{11} and T_{22} are the matrix elements of T. It should be noted that in our calculation, the propagation constant $\beta(= n_{eff}k)$ is complex and has an imaginary part. The imaginary part of β determines the propagation length of the SPP mode (i.e., $L_{spp} = (2\,\mathrm{Im}\,\beta) - 1$), which is related to the Ohmic loss of the metal. In the presence of Ohmic loss, the number of the units that cascaded can affect the transmission of the plasmonic slow light waveguide. By calculating the transmission for different numbers of units, it is found that when the number is 25, the transmission is about 20%, which is high enough for practical applications.

3. Dispersion Tailoring in MIM Waveguide

We first investigate the transmission and dispersion properties of one unit of the grating that coupled to the MIM waveguide by using the transmission line theory. The evolution of transmission spectrum with the distance between the two stubs in a unit is shown in Fig. 2(a). It can be seen that when the distance between the two stubs is zero, there exists two transmitted dips and a transparency peak. The frequencies at the transmitted dips correspond to the resonant frequencies of the two stubs. The appearance of the transparency peak can be attributed to the destructive interference between the electromagnetic fields from the two stubs. The EIT-like transmission spectrum can be easily controlled by tuning the distance between the two stubs. In the following analysis, the distance between two stubs in a unit is chosen as zero (Fig. 1). Besides the distance between the two stubs, the stub depth can also affect the transmission spectrum. As shown in Fig. 2(b), it is found that the transmission spectrum can be tuned by changing stub depth h_2 while maintaining stub depth $h_1 = 220$ nm. From Fig. 2(b), we can draw the following conclusions: when the difference between the two stub depths (i.e., $h_2 - h_1$) increases, EIT-like transmission spectrum becomes more and more obvious. Especially, when the difference between the two stub depths is small, the pass band of the transparency window is narrow, which indicates that a dispersion curve with small slope (i.e., small group velocity) can be obtained. In addition, the frequency at the transparency

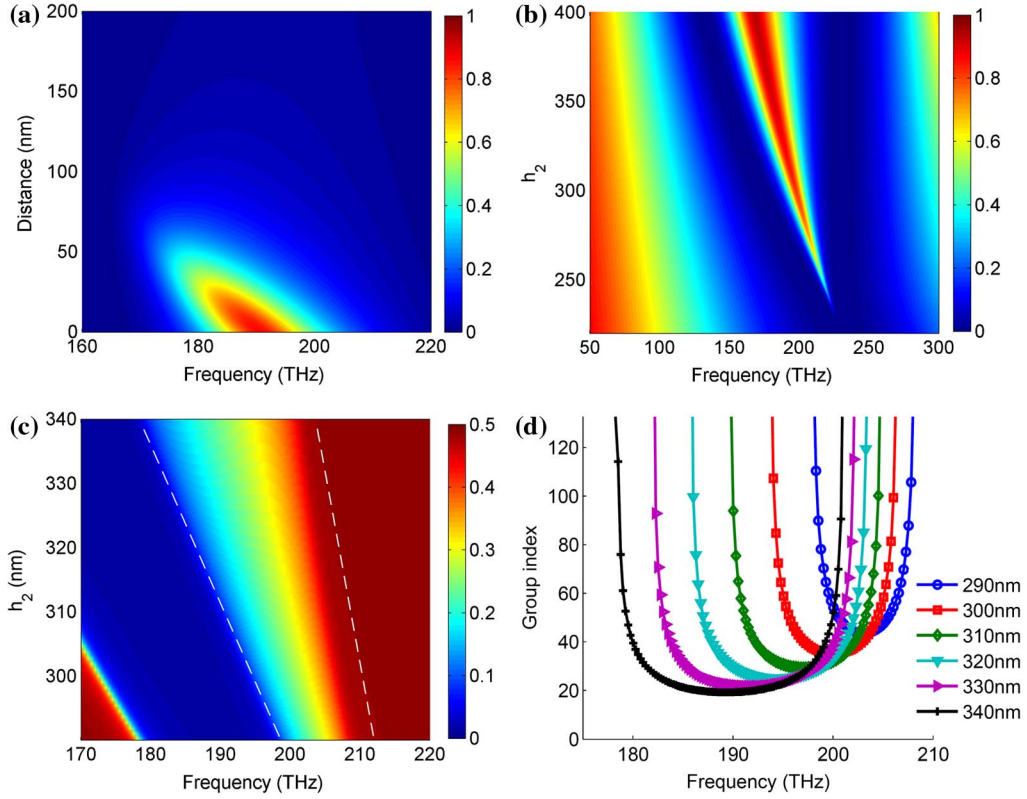

Fig. 2. (Color online) (a) Evolution of transmission spectrum with the distance between the two stubs in one unit of the grating. The width of the waveguide and the stub is $w = 50$ nm and the depths of the two stubs are $h_1 = 220$ nm and $h_2 = 320$ nm, respectively. (b) Evolution of transmission spectrum with h_2. In the calculations, $w = 50$ nm and $h_1 = 220$ nm. (c) Evolution of propagation constant β at different frequencies with the stub depth h_2. The region between the two white dashed lines corresponds to the pass band of the transparency window. (d) Group indices of SPP wave as a function of frequency for different stub depths h_2.

peak has a red-shift with the increase of the stub depth h_2.

To validate the above conclusion, we also calculate the dispersion relationship and the corresponding group indices at different frequencies with the stub depth h_2. In the calculations, the group index is defined as [32]:

$$n_g = c/v_g = cd\beta/d\omega. \tag{4}$$

As shown in Fig. 2(c), it can find that the pass band becomes more and more narrow when you decrease the difference between the two stub depths. Moreover, the frequency at the transparency peak (near the middle of the pass band) has a red-shift with the increase of the stub depth h_2. Figure 2(d) shows the group indices with different stub depth h_2. It can be seen that there is a red-shift of the minimum group index with the increase of stub depth h_2. That is because the frequency at the transparency peak is approximately equal to the first resonant frequency of the composite cavity of length $h_1 + h_2 + w$ formed by the two cavities, where h_1 and h_2 are the stub depths and w is the width of the waveguide [9]. So when the stub depth increases, the frequency at the transparency peak has a red-shift, which results in the red-shift of the minimum group index. It is found that the dispersion analyses are in good agreement with the results in Fig. 2(b). The above results reveal that one can easily control the dispersion relationship by tuning the stub depth.

Successively, we study the relationship between the dispersion properties and the period of the proposed waveguide. As shown in Fig. 3(a), the pass band of the transparency window can be easily tuned by changing the period of the waveguide. Different from tuning the stub depth to engineer the dispersion relationship, the pass band changes almost linearly with the period. In addition, the bandwidth of the pass band and the frequency at the transparency peak change slightly with the period, which are shown in Fig. 3(b). Compared with the stub depth, the period of the waveguide has less impact on the dispersion, even though it still provides an effective way to engineer the dispersion. Especially, the linear relationship between the bandwidth and the period makes it easy to tailor the dispersion.

Based on the above analysis, we investigate and improve the NDBP and reduce the GVD parameter of the proposed slow light waveguide. The concept of NDBP is a good candidate to characterize the compromise between the light slowing down factor and the bandwidth. It is defined as NDBP $\approx \tilde{n}_g(\Delta\omega/\omega)$ [33], and $\tilde{n}_g$ denotes an average group index, which is formulated as:

$$\tilde{n}_g = \int_{\omega_0}^{\omega_0+\Delta\omega} n_g(\omega) \times d\omega/\Delta\omega. \tag{5}$$

From the definition of NDBP, we found that $\tilde{n}_g$ and $\Delta\omega$ determine the NDBP when ω is a fixed. First, we investigate and determine the stub depth to get a high $\tilde{n}_g$. In Fig. 4(a), we show the evolution of transmission spectrum for different stub depths at the frequency of 193.5 THz ($\lambda = 1550$ nm). It is found that only for some stub depths, the transmission of the periodic plasmonic stub waveguide is not zero. According to the former analysis (Fig. 2), we know that when the difference between the two stub depths increases, the group index declines. So according to the results shown in Fig. 4(a), we choose the stub depth as $h_1 = 230$ nm and $h_2 = 300$ nm, respectively. Our chosen can insure the high group index while maintaining high transmission. The NDBP of the proposed structure is not only determined by the group index, but also the bandwidth. Successively, we investigate and obtain a flat dispersion relationship and a large bandwidth while maintaining group index a constant. Especially, the frequency at the transparency peak can keep near 193.5 THz. On the basis of the above analysis (Fig. 3), we know that

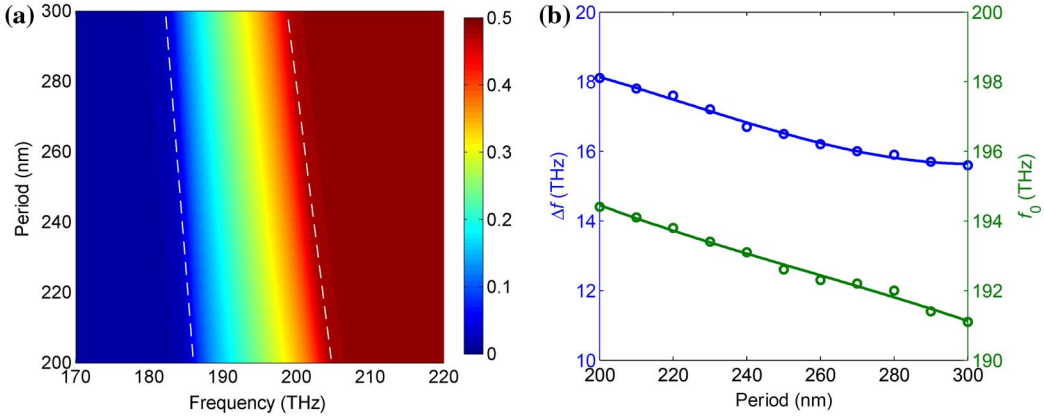

Fig. 3. (Color online) (a) Evolution of propagation constant β at different frequencies with the period p. The region between the two white dashed lines corresponds to the pass band of the transparency window. (b) The bandwidth of the pass band and the frequency at the transparency peak for different periods. The stub depths are $h_1 = 220$ nm and $h_2 = 320$ nm, respectively. The width of the stubs and the waveguide is $w = 50$ nm.

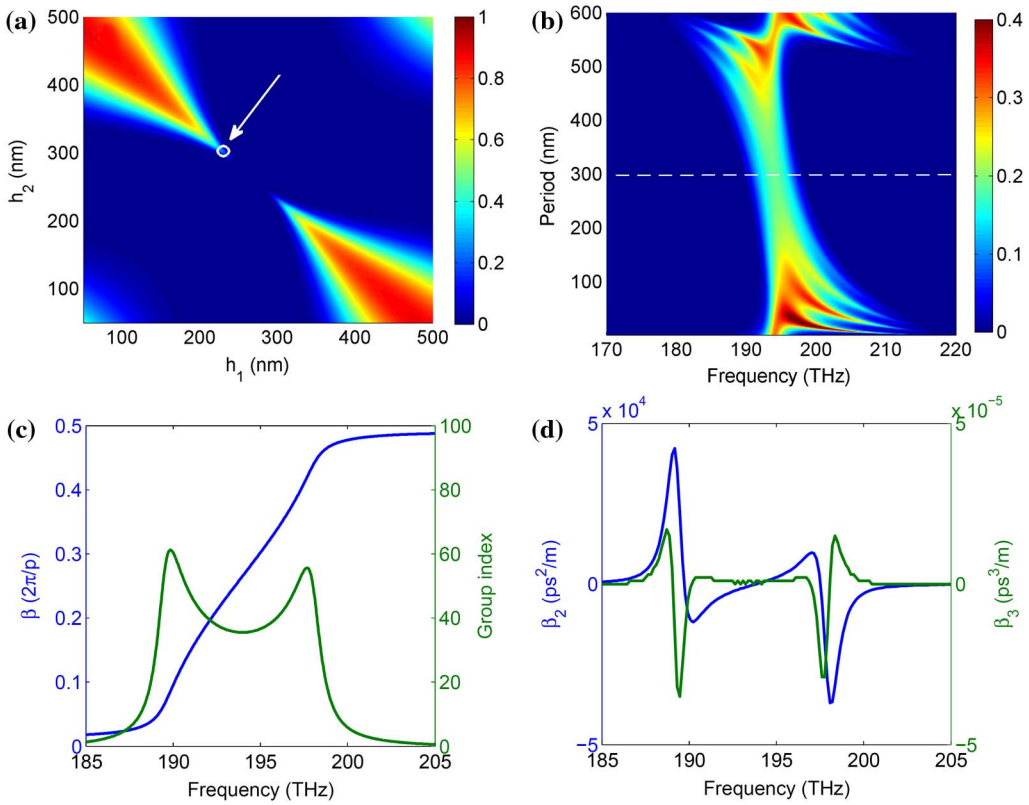

Fig. 4. (Color online) (a) Evolution of transmission spectrum with different stub depths h_1 and h_2 for six units of the grating that coupled to the waveguide. The white circle corresponds to the smallest difference between the two stub depths. The width of the stubs and the waveguide is $w = 50$ nm and the period is $p = 295$ nm. The frequency of the incident light is 193.5 THz. (b) Evolution of transmission spectrum with different p for six units of the grating that coupled to the waveguide. The stub depths are $h_1 = 230$ nm and $h_2 = 300$ nm, respectively. The white line corresponds to the period where the pass band is narrowest. (c) Dispersion relationship and the group index of SPP wave as a function of the frequency. (d) Second- and third-order dispersion parameters of the structure. In calculations of (c)–(d), the parameters are the same as that in (b), except $p = 300$ nm.

the period of the waveguide has less impact on the dispersion relationship. In Fig. 4(b), we calculate the evolution of transmission spectrum with different periods. It can be seen that at the period of 300 nm, the pass band is narrowest, which corresponds to a very flat dispersion curve for the pass band. In our calculations, the group index can be considered to be constant with a $\pm 10\%$ range [34]. In the sense of this criterion, we obtain a flat bandwidth over 3.5 THz and a group index of 35, which is shown in Fig. 4(c). By using Eq. (5) and the definition of NDBP, the NDBP of the waveguide is calculated as 0.65, which is much higher than pervious reports [32]. Compared with Fig. 4(a), p changes from 295 to 300 nm and the frequency for the transparency peak is still near 193.5 THz [according to Fig. 3(b)]. As shown in Fig. 4(c), the proposed waveguide shows "S-shaped" dispersion curve, which indicates that at the inflection point, the GVD parameter equals zero. Here, the second-order dispersion and third-order dispersion (TOD) parameters are characterized by $\beta_2 = d^2k/d\omega^2$ and $\beta_3 = d^3k/d\omega^3 = d\beta_2/d\omega$, respectively. From Fig. 4(d), it can be seen that both the GVD and TOD parameters near the frequency of 193.5 THz equal zero, which implies dispersionless slow light can be obtained in our structure. It should be noted that the proposed flexible waveguide can be designed according to the practical applications. For example, when slow light with a large flat bandwidth is needed, we can appropriately tune the stub depths to make the difference increases. According to Fig. 2(d), when the difference between the two stub depths is large, the dispersion curve becomes very flat and a large flat bandwidth can be achieved. When slow light with large group index is required, the difference between the two stub depths can be chosen a small value. In addition, the role of plasmons in enhancing the group index is also discussed. As we know, when appropriately tuning the difference between the stub depths, the destructive interference between the SPP waves that reflected from the two stubs can result in a very narrow transparency window. The corresponding dispersion curve becomes flat and the slope of that is small. In this way, a significant slow light effect can be realized and a large group index can be enhanced by the destructive interference between the SPP waves.

4. Conclusions

We proposed and theoretically investigate the slow light engineering in periodic plasmonic stub waveguide by using the transmission line theory. The

theoretical results show that the dispersion relationship of the waveguide can be easily tuned by changing the stub depth and the period. Based on the transmission line results, we optimize the parameters of the plasmonic waveguide and a high NDBP of 0.65 can be obtained at the frequency of 193.5 THz and maintaining a large group index of 35. We also find that the proposed structure shows "S-shaped" dispersion curve, which indicates that zero GVD and TOD can be realized at the inflection point of the dispersion curve. The proposed structure has better buffering capacity and can find important applications on optical buffers in highly integrated optical circuits.

This work was supported by the National Natural Science Foundation of China under Grants 10874239, 10604066, and 11204368. The authors acknowledge the fruitful discussions with Dr. Jian Liang.

References

1. M. F. Yanik and S. Fan, "Stopping light all optically," Phys. Rev. Lett. **92** 083901 (2004).
2. M. D. Lukin and A. Imamoglu, "Controlling photons using electromagnetically induced transparency," Nature **413**, 273–276 (2001).
3. M. S. Bigelow, N. N. Lepeshkin, and R. W. Boyd, "Superluminal and slow light propagation in a room-temperature solid," Science **301**, 200–202 (2003).
4. G. Wang, H. Lu, and X. Liu, "Dispersionless slow light in MIM waveguide based on a plasmonic analogue of electromagnetically induced transparency," Opt. Express **20**, 20902–20907 (2012).
5. T. Baba, "Slow light in photonic crystals," Nat. Photonics **2**, 465–473 (2008).
6. J. Liang, L. Ren, M. Yun, X. Han, and X. Wang, "Wideband ultraflat slow light with large group index in a W1 photonic crystal waveguide," J. Appl. Phys. **110**, 063103 (2011).
7. Y. Okawachi, M. S. Bigelow, J. E. Sharping, Z. M. Zhu, A. Schweinsberg, D. J. Gauthier, R. W. Boyd, and A. L. Gaeta, "Tunable all-optical delays via Brillouin slow light in an optical fiber," Phys. Rev. Lett. **94**, 153902 (2005).
8. G. Wang, H. Lu, and X. Liu, "Trapping of surface plasmon waves in graded grating waveguide system," Appl. Phys. Lett. **101**, 013111 (2012).
9. Y. Huang, C. Min, and G. Veronis, "Subwavelength slow-light waveguides based on a plasmonic analogue of electromagnetically induced transparency," Appl. Phys. Lett. **99**, 143117 (2011).
10. L. Yang, C. Min, and G. Veronis, "Guided subwavelength slow-light mode supported by a plasmonic waveguide system," Opt. Lett. **35**, 4184–4186 (2010).
11. H. Lu, X. Liu, and D. Mao, "Plasmonic analog of electromagnetically induced transparency in multi-nanoresonator-coupled waveguide systems," Phys. Rev. A **85**, 053803 (2012).
12. Q. Gan, Y. J. Ding, and F. J. Bartoli, ""Rainbow" trapping and releasing at telecommunication wavelengths," Phys. Rev. Lett. **102**, 056801 (2009).
13. Q. Gan, Z. Fu, Y. J. Ding, and F. J. Bartoli, "Ultrawide-bandwidth slow-light system based on THz plasmonic graded metallic grating structures," Phys. Rev. Lett. **100**, 256803 (2008).
14. G. Wang, H. Lu, and X. Liu, "Gain-assisted trapping of light in tapered plasmonic waveguide," Opt. Lett. **38**, 558–560 (2013).
15. L. Chen, G. Wang, Q. Gan, and F. J. Bartoli, "Trapping of surface-plasmon polaritons in a graded Bragg structure: frequency-dependent spatially separated localization of the visible spectrum modes," Phys. Rev. B **80**, 161106 (2009).
16. G. Wang, H. Lu, X. Liu, D. Mao, and L. Duan, "Tunable multi-channel wavelength demultiplexer based on MIM plasmonic nanodisk resonators at telecommunication regime," Opt. Express **19**, 3513–3518 (2011).
17. H. Lu, X. Liu, Y. Gong, D. Mao, and L. Wang, "Enhancement of transmission efficiency of nanoplasmonic wavelength demultiplexer based on channel drop filters and reflection nanocavities," Opt. Express **19**, 12885–12890 (2011).
18. D. K. Gramotnev and S. I. Bozhevolnyi, "Plasmonics beyond the diffraction limit," Nat. Photonics **4**, 83–91 (2010).
19. Y. Gong, L. Wang, X. Hu, X. Li, and X. Liu, "Broad-bandgap and low-sidelobe surface plasmon polaritons reflector with Bragg-grating-based MIM waveguide," Opt. Express **17**, 13727–13736 (2009).
20. J. Zhang, L. Cai, W. Bai, and G. Song, "Flat surface plasmon polaritons bands in Bragg grating waveguide for slow light," J. Lightwave Technol. **28**, 2030–2036 (2010).
21. G. Wang, H. Lu, X. Liu, and Y. Gong, "Numerical investigation of an all-optical switch in a graded nonlinear plasmonic grating," Nanotechnology **23**, 444009 (2012).
22. H. Lu, X. Liu, L. Wang, Y. Gong, and D. Mao, "Ultrafast all-optical switching in nanoplasmonic waveguide with Kerr nonlinear resonator," Opt. Express **19**, 2910–2915 (2011).
23. H. Lu, X. Liu, D. Mao, L. Wang, and Y. Gong, "Tunable band-pass plasmonic waveguide filters with nanodisk resonators," Opt. Express **18**, 17922–17927 (2010).
24. G. P. Agrawal, *Applications of Nonlinear Fiber Optics*, 4th ed. (Academic, 2007).
25. Y. Gong, X. Liu, and L. Wang, "High channel-count plasmonic filter with the metal–insulator–metal Fibonacci-sequence gratings," Opt. Lett. **35**, 285–287 (2010).
26. J. Park, H. Kim, and B. Lee, "High order plasmonic Bragg reflection in the metal–insulator–metal waveguide Bragg grating," Opt. Express **16**, 413–425 (2008).
27. H. Lu, X. Liu, Y. Gong, D. Mao, and L. Wang, "Optical bistability in MIM plasmonic Bragg waveguides with Kerr nonlinear defects," Appl. Opt. **50**, 1307–1311 (2011).
28. Z. Han, E. Forsberg, and S. He, "Surface plasmon Bragg gratings formed in metal–insulator–metal waveguides," IEEE Photon. Technol. Lett. **19**, 91–93 (2007).
29. H. Lu, X. Liu, Y. Gong, L. Wang, and D. Mao, "Multi-channel plasmonic waveguide filters with disk-shaped nanocavities," Opt. Commun. **284**, 2613–2616 (2011).
30. A. Pannipitiya, I. D. Rukhlenko, M. Premaratne, H. T. Hattori, and G. P. Agrawal, "Improved transmission model for metal–dielectric–metal plasmonic waveguides with stub structure," Opt. Express **18**, 6191–6204 (2010).
31. J. Liu, G. Fang, H. Zhao, Y. Zhang, and S. Liu, "Surface plasmon reflector based on serial stub structure," Opt. Express **17**, 20134–20139 (2009).
32. R. Hao, E. Cassan, X. Le Roux, D. Gao, V. Do Khanh, L. Vivien, D. Marris-Morini, and X. Zhang, "Improvement of delay-bandwidth product in photonic crystal slow-light waveguides," Opt. Express **18**, 16309–16319 (2010).
33. R. Hao, E. Cassan, H. Kurt, X. Le Roux, D. Marris-Morini, L. Vivien, H. Wu, Z. Zhou, and X. Zhang, "Novel slow light waveguide with controllable delay-bandwidth product and ultra-low dispersion," Opt. Express **18**, 5942–5950 (2010).
34. L. H. Frandsen, A. V. Lavrinenko, J. Fage-Pedersen, and P. I. Borel, "Photonic crystal waveguides with semi-slow light and tailored dispersion properties," Opt. Express **14**, 9444–9450 (2006).